Substrate-Assisted Crystallization and Photocatalytic Properties of Mesoporous TiO_2 Thin Films

Yu Zhang,[†] Jun Li,[‡,§] and John Wang*[,†]

Department of Materials Science and Engineering, Faculty of Engineering, National University of Singapore, Singapore 117576, and Division of Bioengineering, Faculty of Engineering, NUS and Institute of Materials Research and Engineering (IMRE), Singapore 117602

Received February 23, 2006. Revised Manuscript Received April 11, 2006

Highly crystallized mesoporous TiO_2 thin films with enhanced photocatalytic activity were synthesized via a substrate-assisted strategy. Three types of substrates, namely, amorphous glass, polycrystalline Pt, and single-crystal Si(111) wafer, were employed to study their effects on the structure of TiO_2 films, by using small-angle X-ray scattering (SAXS), transmission electron microscopy (TEM), X-ray diffraction (XRD), a Raman spectrometer, and a UV−vis spectrophotometer. When the substrate was changed from amorphous glass to polycrystalline Pt and then to single-crystal Si(111), a transition in the pore configuration took place from a cubical configuration to cagelike arrays, accompanied by an increase in nanocrystallinity. The observed transitions in pore configuration of mesoporous TiO_2 can be accounted for by the differences in nucleation behaviors and surface energy among the substrate systems involved. Mesoporous TiO_2 thin films of enhanced nanocrystallinity demonstrate improved photocatalytic activity for degradation of methylene blue (MB) under UV irradiation. They also show photoluminescence at room temperature, which is related to the radiative recombination of excitons.

Introduction

TiO_2-based mesoporous structures with pores between 2 and 50 nm have attracted much attention, owing to their excellent functional properties for various technologically important applications, such as in solar energy conversion, batteries, and photocatalysis.[1−3] They were first prepared by using alkyl phosphate anionic surfactant as the template by Antonelli et al.[4] However, a significant amount of phosphates remained in the resulting mesoporous structure, which underwent partial collapse when the template was removed by calcination at elevated temperatures. A couple of other templates have also been attempted, including the quaternary ammonium cationic templates,[5] primary amines,[6] and poly(ethylene oxide) (PEO)-based surfactants.[7] Evaporation-induced self-assembly (EISA) was then adopted by Stucky et al,[8] to synthesize mesoporous transition-metal oxide powders. Indeed, it has since been used for preparation of mesoporous structures in several systems. Transparent mesoporous TiO_2 thin films with a well-organized hexagonal, mesoporous structure was realized by further extending the EISA approach.[9]

To synthesize and understand TiO_2-based mesoporous materials, on the one hand, several relationships between the various synthesis parameters, such as pH,[10] moisture,[11] and water content,[12] and the resulting nanostructures have been established. They help to realize the desired mesoporous structures of large specific surface area and high porosity level in controlled configurations. On the other hand, however, most of these previous studies are limited to the mesoporous structures of low crystallinity. Realization of mesoporous TiO_2 thin films with enhanced nanocrystallinity is required by several technologically demanding applications, such as for photocatalysis,[13] where the semiconducting and photovoltaic behaviors are largely dependent on the crystallinity of TiO_2. Unfortunately, crystallization in an uncontrolled manner by conventional thermal treatment often leads to collapse of the mesoporous TiO_2 network due to the extensive growth of nanocrystals at the sacrifice of specific surface area.[14] Therefore, it is very important to understand the crystallization process of mesoporous TiO_2,

* To whom correspondence should be addressed. Phone: +65 65161268. Fax: +65 67763604. E-mail: msewangj@nus.edu.sg.

[†] Department of Materials Science and Engineering, Faculty of Engineering, National University of Singapore.

[‡] Division of Bioengineering, Faculty of Engineering, National University of Singapore.

[§] Institute of Materials Research and Engineering, Singapore.

(1) Stone, V. F.; Davis, R. J. *Chem. Mater.* **1998**, *10*, 1468.
(2) Perez, M. D.; Otal, E.; Bilmes, S. A.; Soler-Illia, G. J.; Crepaldi, E. L.; Grosso, D.; Sanchez, C. *Langmuir* **2004**, *20*, 6879.
(3) Idakiev, V.; Tabakova, T.; Yuan, Z. Y.; Su, B. L. *Appl. Catal., A* **2004**, *270*, 135.
(4) Antonelli, D. M.; Ying, J. Y. *Angew. Chem., Int. Ed. Engl.* **1995**, *34*, 2014.
(5) Soler-Illia, G. J.; Louis, A.; Sanchez, C. *Chem. Mater.* **2002**, *14*, 750.
(6) Wang, Y. Q.; Tang, X. H.; Yin, L. X.; Huang, W. P.; Hacohen, Y. R.; Gedanken, A. *Adv. Mater.* **2000**, *12*, 1183.
(7) Yang, P. D.; Zhao, D. Y.; Margolese, D. I.; Chmelka, B. F.; Stucky, G. D. *Chem. Mater.* **1999**, *11*, 2813.
(8) Yang, P. D.; Zhao, D. Y.; Margolese, D. I.; Chmelka, B. F.; Stucky, G. D.; *Nature* **1998**, *396*, 152.
(9) Yun, H. S.; Miyazawa, K.; Zhou, H. S.; Honma, I.; Kuwabara. M. *Adv. Mater.* **2001**, *13*, 1377.
(10) Li, X. S.; Fryxell, G. E.; Birnbaum, J. C.; Wang, C. M. *Langmuir* **2004**, *20*, 9095.
(11) Jang, K. S.; Song, M. G.; Cho, S. H.; Kim, J. D. *Chem. Commun.* **2004**, 1514.
(12) Crepaldi, E. L.; Soler-Illia, G. J.; Grosso, D.; Cagnol, F.; Ribot, F.; Sanchez, C. *J. Am. Chem. Soc.* **2003**, *125*, 9770.
(13) Hoffmann, M. R.; Martin, S. T.; Choi, W. Y.; Bahnemann, D. W. *Chem. Rev.* **1995**, *95*, 69.
(14) Crepaldi, E. L.; Soler-Illia, G. J.; Grosso, D.; Sanchez, C. *New J. Chem.* **2003**, *27*, 9.

10.1021/cm060450b CCC: $33.50
Published on Web 05/18/2006

to achieve the most desirable pore configuration with much enhanced nanocrystallinity.

Indeed, several approaches have been taken to increase the nanocrystallinity of TiO_2-based mesoporous structures. For example, PEO−poly(propylene oxide) block copolymers were used, instead of surfactants of small molecules as templates, resulting in much thicker titania walls capable of embracing relatively large nanocrystals.[15,16] Poly(ethylene-co-butylene)-*b*-PEO was also developed, to control the pore size such that a robust titania gel structure can be supported.[17] Thermal stability of mesoporous TiO_2 films was successfully improved to 700 °C by carefully delaying the rapid crystallization.[18] Supercritical fluid processing was also employed, to realize a mesoporous titania structure with remarkable high thermal stability that can support nucleation and crystal growth.[19,20]

Moreover, for thin films, their texture development and nanocrystallinity can be strongly affected by the nature and characteristics of the substrate, where the interface between the substrate and thin film can involve a number of phenomena, such as epitaxy, residual stress and strain, and interfacial energies.[21,22] By taking a different approach in this paper, we have explored the effects of substrate type on the pore configuration and nanocrystallinity of mesoporous TiO_2 thin films, when surfactant templating is employed to realize the mesoporous structures. Indeed, as detailed below, both mesopore configurations and nanocrystallinity of TiO_2 thin films can be strongly affected, when the substrate is changed from amorphous glass to polycrystalline Pt and then to single-crystal Si(111) wafer. In particular, polycrystalline Pt and single-crystal Si(111) wafer can lead to a highly crystallized mesoporous TiO_2 film with anatase nanoparticles embedded in the framework at a temperature of as low as 350 °C. The photocatalytic activity of these mesoporous TiO_2 films using methylene blue (MB) as a photocatalytic reactant was investigated. The effectiveness of photocatalytic reactions was proven to be strongly dependent on the porosity, the specific surface area, and more importantly the nanocrystallinity of titania. In addition, the mesoporous films of enhanced nanocrystallinity demonstrate photoluminescence (PL) at room temperature, arising from recombination of electron/hole pairs, which has never been reported for mesoporous TiO_2 thin films without proper dopants.

Experimental Section

Preparation of Mesoporous TiO_2 Thin Films. Mesoporous TiO_2 thin films were prepared at room temperature by following the procedures described below: a precursor solution was first prepared by mixing appropriate amounts of ethanol, hydrochloric acid (HCl), titanium tetraisopropoxide (TTIP, Aldrich, 97%), acetyl acetone (AcAc), and deionized water (H_2O) and then stirred for 2 h. Triblock copolymer Pluronic F127 (designated $EO_{106}PO_{70}EO_{106}$, BASF) was then dissolved in ethanol and then mixed with the precursor solution. Molar ratios of the ingredients were controlled as follows: TTIP/F127/AcAc/HCl/H_2O/ethanol = 1:0.004:0.5:0.5:15:40. After being stirred for 3 h more, the sol solution thus obtained was deposited on three different substrates, namely, amorphous glass substrate, polycrystalline Pt substrate, and single-crystal Si(111) wafer by spin coating (3000 rpm for 1 min). A gentle heating was then applied to enhance the inorganic polymerization and stabilize the mesophases involved, typically at 40 °C (48 h) and then 110 °C (24 h) in air. Finally, the organic template was removed by calcination in air at 350 °C (4 h, 1 °C min^{-1} ramp).

Characterization. Two-dimensional small-angle X-ray scattering (SAXS) patterns for the resulting TiO_2 films were obtained by using a Bruker AXS Nanostar SAXS System, with Cu Kα radiation (1.54 Å), operated at 40 kV and 35 mA. Both transmission electron microscopy (TEM; JEOL JEM 2010F, 200 kV) and high-resolution TEM (HRTEM; JEOL JEM 3010, 300 kV) were employed to study the morphology and texture of the mesoporous TiO_2 films. Nanocrystallites of the anatase phase in the mesoporous thin films were characterized using a Raman spectrometer (U1000 Jobin-Yvon double monochromator) and X-ray diffraction (XRD; Bruker AXS D8 Advance, Germany). Their PL emission spectra were measured using a Raman spectrometer with a 325 nm He−Cd laser as the excitation light source.

Photocatalytic Activity Measurements. Photocatalytic decomposition of MB with mesoporous TiO_2 films deposited on different substrates was examined. The films were scratched off the substrates and put in a 4 mL spectrophotometer quartz cuvette containing 3 mL 10^{-5} M MB aqueous solution in air, before the cuvette was sealed with a telfon stopper. The area of the titania films scratched off the substrates for testing was fixed at 8 cm^2, with an average thicknesses of 135 ± 7, 133 ± 7, and 145 ± 8 nm for the films deposited on Si(111), Pt, and glass substrates, respectively. The cuvette was then stored in the dark for 90 min until the absorption remained constant. The UV light was provided by a 4 W germicidal lamp (λ_{max} = 253.7 nm, G4T5). The distance between the lamp and the cuvette was controlled at 4 cm. Change of the MB concentration as a function of the absorption of the solution at 664 nm (A_{664}) was monitored using a UV−vis spectrophotometer (UV-1601, Shimadzu) with a 30 min interval for a total irradiation time of 300 min.

Results and Discussion

Morphology and Phase Evolution of Mesoporous TiO_2 Thin Films. Figure 1 shows SAXS patterns of the mesoporous TiO_2 thin films deposited on amorphous glass substrate, polycrystalline Pt substrate and single-crystal Si(111) wafer, respectively, after calcination at 350 °C. There was no significant change in the position of the (110) diffraction peak, when the substrate was changed from amorphous glass to polycrystalline Pt and then to single-crystal Si(111). However, the peak intensity for the film deposited on the Si(111) wafer was much reduced, indicating that the ordered mesoporous structure had undergone some degradation, as compared to those of the thin films deposited on amorphous glass and polycrystalline Pt.

TEM as a local probing technique provides more detailed information on the mesostructure of the three TiO_2 films.

(15) Grosso, D.; Soler-Illia, G. J.; Babonneau, F.; Sanchez, C.; Albouy, P. A.; Brunet-Bruneau, A.; Balkenende, A. R. *Adv. Mater.* **2001**, *13*, 1085.
(16) Alberius, P. C. A.; Frindell, K. L.; Hayward, R. C.; Kramer, E. J.; Stucky, G. D.; Chmelka, B. F. *Chem. Mater.* **2002**, *14*, 3284.
(17) Smarsly, B.; Grosso, D.; Brezesinski, T.; Pinna, N.; Boissiere, C.; Antonietti, M.; Sanchez, C. *Chem. Mater.* **2004**, *16*, 2948.
(18) Grosso, D.; Soler-Illia, G. J.; Crepaldi, E. L.; Cagnol, F.; Sinturel, C.; Bourgeois, A.; Brunet-Bruneau, A.; Amenitsch, H.; Albouy, P. A.; Sanchez, C. *Chem. Mater.* **2003**, *15*, 4562.
(19) Wang, K. X.; Morris, M. A.; Holmes, J. D. *Chem. Mater.* **2005**, *17*, 1269.
(20) Wang, K. X.; Yao, B. D.; Morris, M. A.; Holmes, J. D. *Chem. Mater.* **2005**, *17*, 4825.
(21) Yang, H. G.; Zeng, H. C. *J. Phys. Chem. B* **2003**, *107*, 12244.
(22) Chougnet, A.; Heitz, C.; Sondergard, E.; Berquier, J. M.; Albouy, P. A.; Klotz, M. *J. Mater. Chem.* **2005**, *15*, 3340.

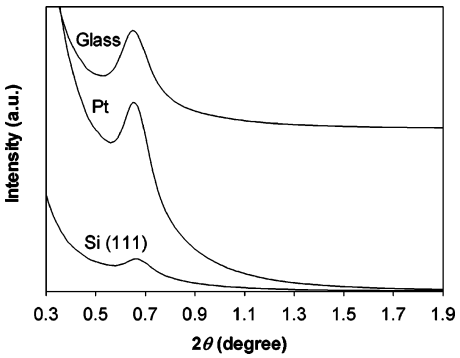

Figure 1. SAXS patterns of the mesoporous TiO_2 thin films deposited on three different substrates, namely, amorphous glass, polycrystalline Pt substrate, and single-crystal Si(111) wafer, after calcination at 350 °C.

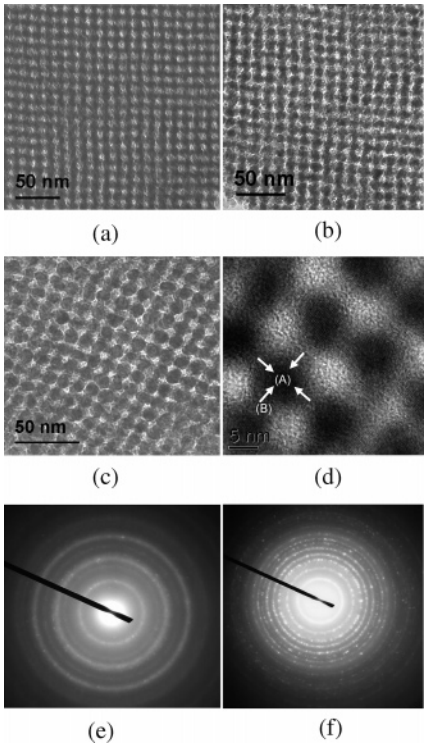

Figure 2. TEM images of the mesoporous TiO_2 thin films deposited on (a) amorphous glass, (b) polycrystalline Pt, and (c) single-crystal Si(111) wafer; (d) HRTEM image of the TiO_2 thin film deposited on polycrystalline Pt; (e and f) are the SAD patterns of parts b and c, respectively.

Compared with the cubical configuration of discrete mesopores for the film deposited on the amorphous glass substrate (Figure 2a), polycrystalline Pt, and single-crystal Si(111) substrates led to a cagelike pore configuration, where the mesopores became more interconnected and surrounded by titania nanoparticle islands (Figure 2b,c). The selected area diffraction (SAD pattern, Figure 2e) reveals that the TiO_2 film deposited on polycrystalline Pt substrate was partially crystallized with the anatase phase. A much further enhanced nanocrystallinity is shown for the TiO_2 film deposited on the Si(111) wafer, as evidenced by the well-established diffraction pattern (Figure 2f). Admittedly, crystallization often degrades the mesopore structure, leading to partial contraction of mesopores and even collapse of the local titania network. Studies using HRTEM of the film deposited on polycrystalline Pt substrate (Figure 2d) confirms the formation of anatase nanocrystals with a quantum dotlike arrangement embedded in the mesopore arrays. Their average size, as evaluated by studying 200 nanoparticles, is 8.8 ± 0.8 nm, which is slightly smaller than that of the TiO_2 film deposited on the Si(111) wafer (10.8 ± 1.3 nm).

Shown in Figure 3a are the Raman spectra of the mesoporous TiO_2 thin films deposited on the three substrates. Obviously, no clear crystalline phase was formed on the amorphous glass substrate at 350 °C. In contrast, well-established bands at 148, 201, 403, 522, and 644 cm^{-1}, which are characteristic bands of the anatase phase,[23] were observed for those deposited on the polycrystalline Pt and single-crystal Si(111) substrates.

Figure 3b−d plots the change in frequency and peak width of the E_g mode for TiO_2 thin films deposited on the three substrates, respectively, where the full curves represent the fitting results and the dots are for the experimental data. There occurred a red shift in frequency and a decrease in width of the lowest frequency E_g mode from amorphous glass to polycrystalline Pt and then to single-crystal Si(111) wafer, with full widths at half-maximum (fwhm) of 35.37, 17.47, and 14.60 cm^{-1} and frequencies of 151.77, 148.43, and 145.16 cm^{-1}, respectively. It is well-understood that a refinement in crystallite size to the nanometer range, together with a high density of defects in thin films, which is closely related to the degree of nanocrystallinity, can lead to a frequency shift and asymmetry broadening of Raman peaks. In the present study, the red shift and narrowing of the E_g mode with increasing TiO_2 crystallite size from glass to Pt and then to Si(111) systems can be accounted for by a combined mechanism involving phonon confinement and nonstoichiometry effects.[23,24] This is supported by what has been shown by electron diffraction of TEM studies, where there is an apparent enhancement in the nanocrystallinity of the anatase phase for the films deposited on the Si(111) wafer and Pt substrate, as compared to that deposited on amorphous glass.

Figure 4 shows the XRD spectra for the mesoporous thin films deposited on the three substrates, namely, amorphous glass, polycrystalline Pt, and single-crystal Si(111) wafer. Both polycrystalline Pt and single-crystal Si(111) wafer gave rise to well-established peaks of the anatase phase, which can be ascribed to the (101), (004), (200), (105), (211), and (204) planes. The fwhm of the (101) peak was further obtained by fitting to a Gaussian distribution (Figure 5), where the calculation of the peak width using the Scherrer equation yielded an average crystallite sizes of 8.2 and 9.8 nm for the mesoporous TiO_2 films deposited on polycrystalline Pt substrate and single-crystal Si(111) wafer, respectively. They are in excellent agreement with what were obtained from the TEM studies, confirming that the film deposited on the Si(111) wafer exhibited the highest crystallinity and the largest crystallite size.

On the basis of the discussion above, the effects of substrate type in promoting crystallization can be summarized as single-crystal Si(111) wafer > polycrystalline Pt substrate

(23) Zhang, W. F.; He, Y. L.; Zhang, M. S.; Yin, Z.; Chen, Q. *J. Phys. D: Appl. Phys.* **2000**, *33*, 912.
(24) Kolobov, A. V.; Wei, S. Q.; Yan, W. S.; Oyanagi, H.; Maeda, Y.; Tanaka, K. *Phys. Rev. B* **2003**, *67*, 195314.

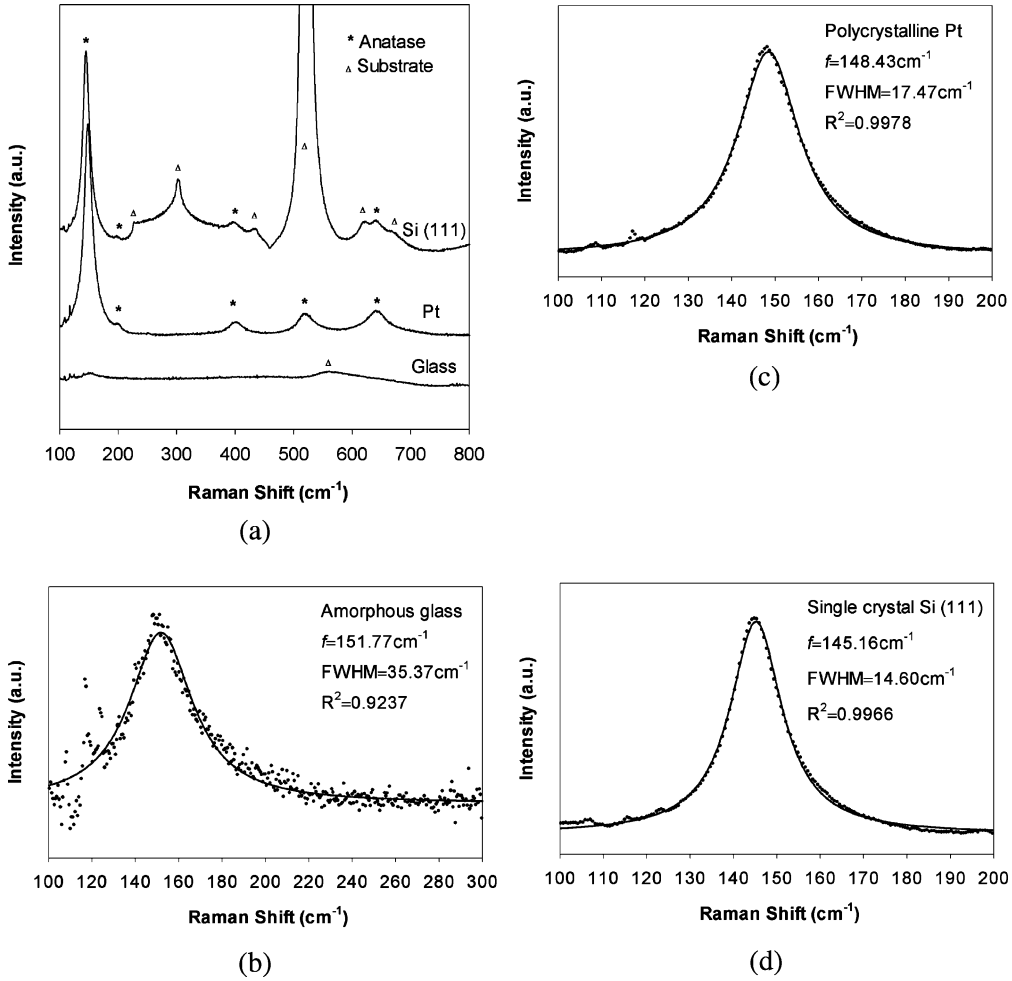

Figure 3. (a) Raman spectra of the mesoporous TiO_2 thin films deposited on the three substrates, after calcination at 350 °C; (b−d) the full curves are fit to a Lorentzian distribution.

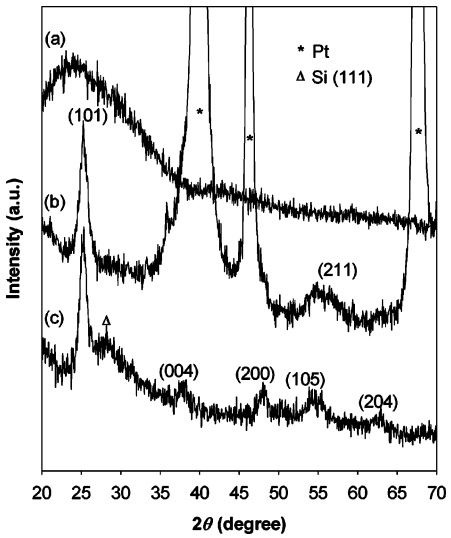

Figure 4. XRD spectra of the mesoporous TiO_2 thin films deposited on (a) amorphous glass, (b) polycrystalline Pt, and (c) single-crystal Si(111), respectively, after calcination at 350 °C.

> amorphous glass substrate. Apparently, the single-crystal Si(111) wafer, which exhibits a highly ordered crystal structure on the surface, can significantly facilitate crystallization of the mesoporous titania thin film.[25] This is followed by polycrystalline Pt, while amorphous glass has the least effect. Studies of surface roughness also support the fact that both Si(111) and Pt promoted crystallization of the mesoporous TiO_2 thin film. For example, surface roughnesses of 0.783, 1.463, and 1.493 nm were measured for the mesoporous films deposited on amorphous glass, polycrystalline Pt, and single-crystal Si(111) wafer, respectively. Undoubtedly, crystal growth had increased the surface roughness, when polycrystalline Pt and single-crystal Si(111) wafer were used as the substrates for depositing mesoporous TiO_2 thin films.

A mechanism is thus proposed to explain the morphology change and phase evolution in mesoporous TiO_2 thin films as affected by the three types of substrates. First, both single-crystal Si(111) wafer and polycrystalline Pt substrate exhibit a more ordered structure than that of amorphous glass. Therefore, they can offer sites for heterogeneous nucleation, which reduces the energy barrier to nucleate.[26] Thus, a relatively low temperature is required to rearrange atoms in the local scales to form crystallites for subsequent crystal growth. In the presence of a mesoporous structure, however, the pore network disfavors formation of an ideal crystal structure in extended three dimensions. Therefore, small crystallites will first nucleate within the walls of the

(25) Debbagh, F.; Ameziane, E. L.; Azizan, M.; Outzourhit, A.; Brunel, M. *Phys. Status Solidi A* **1996**, *157*, 19.
(26) Brar, T.; France, P.; Smirniotis, P. G. *J. Phys. Chem. B* **2001**, *105*, 5383.

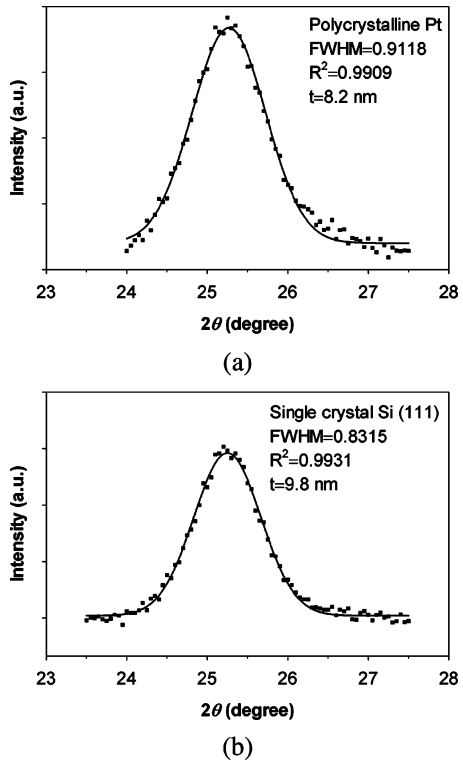

Figure 5. Line shapes of the (101) diffraction peak of mesoporous TiO_2 thin films deposited on (a) polycrystalline Pt and (b) single-crystal Si(111), respectively. The full curves are fit to a Gaussian distribution.

mesoporous structure. To further reduce the total energy of the system, the small crystallites tend to grow into large ones, by increasing their volume to surface area ratios. This inevitably involves transportation of titania species from neighboring sites. As shown in Figure 2d, site A, owing to its large wall space, allowing crystallites to grow to bigger size would be a more energetically favored position for titania species to diffuse to than site B. Continuation of this process will cause the merge of some adjacent mesopores through the neck. Crystallization from an initial amorphous framework will eventually lead to the loss of some local connections of the initial titania framework and, therefore, the rearrangement of the mesopore configuration. On the other hand, the spatial confinement by pore arrays will slow the process, leading to a more or less uniform distribution of titania nanocrystals as shown by the TEM micrograph in Figure 2. Further growth of the nanocrystals will inevitably lead to contraction of pores and loss of ordering. The driving force for the process is the apparent minimization of the surface energy in association with the formation and crystal growth of the anatase phase. Crystallization at a lowered temperature will be beneficial to preservation of the mesoporous structure. A cagelike configuration with more or less uniformly sized TiO_2 quantum dot structure is established, in the cases of polycrystalline Pt and single-crystal Si(111) wafer.

Photocatalytic Properties of Mesoporous TiO_2 Thin Films. Photocatalytic performance of the mesoporous TiO_2 thin films deposited on the three substrates was evaluated for degrading MB under UV irradiation. Figure 6a shows the variation in absorption of MB at 664 nm for the titania films as a function of exposure time, which was used to

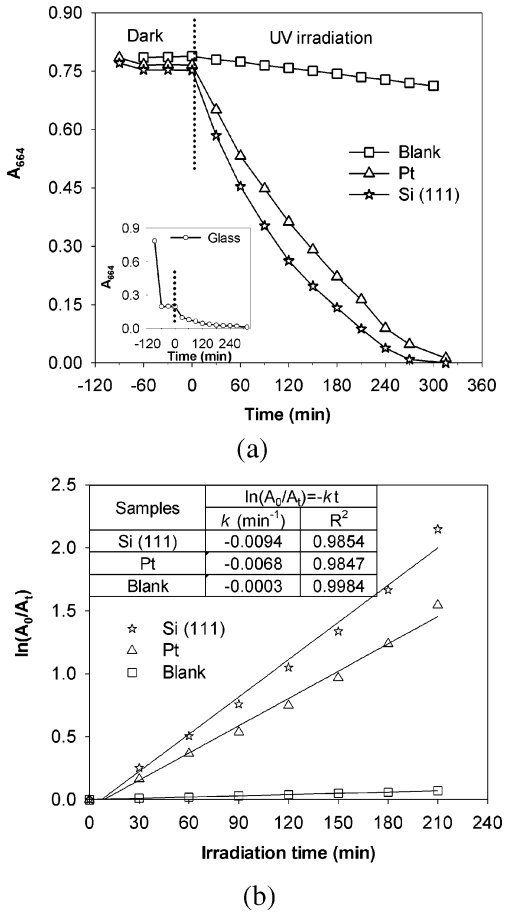

Figure 6. (a) Changes in MB concentrations as a function of exposure time. (b) First-order linear relation when the UV irradiation time was less than 210 min and determination of the apparent first-order degradation rate constant, *k*.

estimate the change in the concentration of MB as the photocatalytic reaction proceeded, based on the linear relationship between the concentration and the absorption of MB according to the Lambert−Beer equation. The blank test confirms that MB was not degraded in the dark and only slightly degraded under UV light in the absence of catalysts. For the films deposited on polycrystalline Pt substrate and Si(111) wafer, physical adsorption of MB occurs and reaches saturation in less than 30 min. After that, the concentrations of MB were scarcely observed to change until the UV irradiation was started. The concentrations of MB decreased quickly with increasing UV irradiation time, and the photocatalytic activity of the mesoporous TiO_2 film deposited on Si(111) wafer is higher than that of the film deposited on Pt substrate, which is related to the higher nanocrystallinity of the former.

A plot of $\ln(A_0/A)$ versus irradiation time was presented in Figure 6b, as a straight line, when the UV irradiation time was less than 210 min. It indicates that the photodegradation of MB obeys pseudo-first-order kinetics over this time period and the slope equals the apparent degradation rate constant (k), in agreement with the generally observed Langmuir−Hinshelwood mechanism.[27] For the mesoporous thin films deposited on single-crystal Si(111) wafer and polycrystalline Pt, the k is calculated as $k_{Si(111)} = -9.4 \times 10^{-3}$ min^{-1} and

(27) Yu, J. C.; Wang, X. C.; Fu, X. Z. *Chem. Mater.* **2004**, *16*, 1523.

$k_{Pt} = -6.8 \times 10^{-3}$ min^{-1} and the half-life ($t_{1/2}$) is $t_{1/2,Si(111)} = 73.7$ min and $t_{1/2,Pt} = 101.9$ min, respectively.

However, the film deposited on glass substrate exhibits rather different absorption and catalysis behaviors (Figure 6a, inset). First, there was change in color in the MB solution from blue to indigo upon addition of the TiO_2 film scratched off the glass substrate. The absorption of MB at 664 nm in the UV−vis spectra decreased sharply (by 75%) in less than 30 min correspondingly. The observed change in color suggests that a strong physical absorption and a degree of chemical interaction, such as the dimerization process of MB,[28] occurred between the catalyst and the MB even before the UV irradiation. That means the sharp decrease in absorption of MB in the UV−vis spectra corresponded to a transformation of MB to other molecular forms and absorption on titania, instead of a real degrading process of organic reactants. Upon UV irradiation, the MB solution slowly turned from indigo to violet, and the violet color did not disappear within the irradiation time conducted. They were shown to be thionine or other *N*-demethylated intermediates of MB.[29] This is in contrast to the films deposited on polycrystalline Pt substrate and single-crystal Si(111) wafer, which are able to completely decompose the MB to a colorless solution within the experiment time conducted.

Upon contact with the TiO_2 thin films, MB molecules will diffuse into the mesoporous structure and adsorb on the mesopore surfaces. Electrons and holes generated by irradiation with UV light in the mesoporous TiO_2 will migrate to the surfaces, where they are captured by reductants (e.g., H_2O) and oxidants (e.g., O_2), producing active radical species. These active species react with MB molecules adsorbed on the mesopore surface, resulting in their decomposition. For the film deposited on glass substrate, on the one hand, the absorption was promoted by the observed mesopore structure and large specific surface area. However, the structural randomness in association with the amorphous nature of titania lowers the efficiency to prevent the electron−hole recombination, and thus a negligible photocatalytic activity was observed, where the low degradability for organic reactants is unable to completely mineralize them into CO_2 and H_2O. In contrast, the mesoporous TiO_2 films deposited on the polycrystalline Pt substrate and single-crystal Si(111) wafer showed a remarkable improvement of the photoreactivity arising from their enhanced nanocrystallinity.

Photoluminescence Behaviors of Mesoporous TiO_2 Thin Films. TiO_2, as an indirect band gap semiconductor, often lacks luminescence under normal conditions, although it has demonstrated some luminescence behaviors, for example, in a vacuum environment,[30] at very low temperature ($T = 77$ K),[31] in the presence of dopants,[31] and in ultrafine TiO_2 colloidal solution form ($d \approx 3$ nm).[32] As a result of the amorphous titania structure, the mesoporous film deposited on glass substrate shows no PL at room temperature. In contrast, PL behaviors were observed with the mesoporous TiO_2 thin films deposited on polycrystalline Pt substrate and single-crystal Si(111) wafer in the present work. Figure 7 shows their PL behaviors under excitation with $\lambda = 325$ nm in air at room temperature. The broad band at 440−560 nm (2.20−2.80 eV) in the visible range is associated with the radiative recombination of excitons due to shallow traps identified with oxygen vacancy and Ti^{4+} adjacent to oxygen vacancies.[33,34] In addition, there is a broad band at 670−710 nm (1.75−1.85 eV), which is considered to be a consequence of the transitions of electrons from the conduction band to valence band holes, trapped at an interstitial Ti^{3+} site.[32] Careful comparison of luminescence band intensities shows that the film deposited on single-crystal Si(111) wafer exhibits a higher density of shallow traps such as oxygen vacancies, while the film deposited on the Pt substrate exhibits more interstitial Ti^{3+} defects.

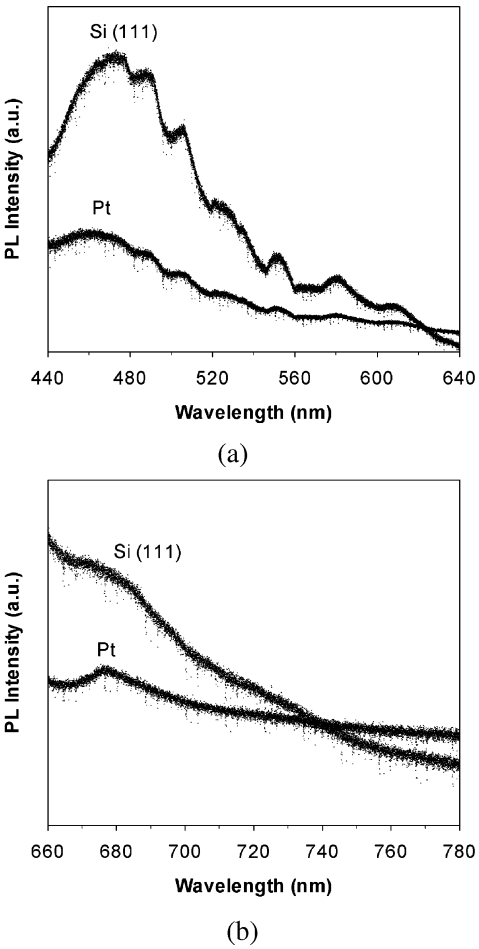

Figure 7. PL spectra of the mesoporous TiO_2 thin films deposited on polycrystalline Pt substrate and single-crystal Si(111) wafer, in the wavelength range of (a) 440−640 nm and (b) 660−780 nm.

The observed PL with the mesoporous anatase thin films is not related to any specific impurity. Instead, it is assigned to the transitions from intragap energy levels implicating lattice and/or surface defects in association with nanoparticles. Given the cagelike mesostructure and the large surface

(28) Mills, A.; Wang, J. S. *J. Photochem. Photobiol., A* **1999**, *127*, 123.
(29) Zhang, T. Y.; Oyama, T.; Aoshima, A.; Hidaka, H.; Zhao, J. C.; Serpone, N. *J. Photochem. Photobiol., A* **2001**, *140*, 163.
(30) Forss, L.; Schubnell, M. *Appl. Phys. B* **1993**, *56*, 363.
(31) Tang, H.; Berger, H.; Schmid, P. E.; Levy, F. *Solid State Commun.* **1993**, *87*, 847.
(32) Liu, Y. J.; Claus, R. O. *J. Am. Chem. Soc.* **1997**, *119*, 5273.
(33) Serpone, N.; Lawless, D.; Khairutdinov, R. *J. Phys. Chem.* **1995**, *99*, 16646.
(34) Dong, W. J.; Pang, G. S.; Shi, Z.; Xu, Y. H.; Jin, H. Y.; Shi, R.; Ma, J. J.; Feng, S. H. *Mater. Res. Bull.* **2004**, *39*, 433.

area of nanocrystallites, one would expect a great number of defects on the nanocrystal surfaces available to trap the electrons when the electrons are excited to the conduction band. These surface defects, or traps, are assigned to coordinatively unsaturated titanium ions or oxygen vacancies on the surfaces. The defect energy levels can act as a separation center. For example, Ti^{3+} was reported to be able to enhance the oxygen chemisorption and promote the excited electrons trapped by O_2.[35] This can contribute to the observed high activity in photodegradation of MB by the mesoporous TiO_2 films deposited on the polycrystalline Pt substrate and single-crystal Si(111) wafer.

Conclusions

Both the pore configuration and the nanocrystallinity of mesoporous TiO_2 thin films are strongly affected by the types of substrate, when surfactant templating is used to deposit the mesoporous thin films. Among the three substrates studied in the present work, namely, amorphous glass, polycrystalline Pt, and single-crystal Si(111) wafer, the mesoporous TiO_2 thin film deposited on single-crystal Si(111) wafer exhibited the highest nanocrystallinity, upon calcination at 350 °C, as shown by studies using TEM, Raman scattering, and XRD. This is followed by the mesoporous TiO_2 thin film deposited on the polycrystalline Pt substrate, while little crystallinity is observed with the amorphous glass substrate. There is a transition in the pore configuration, from a cubical array of discrete pores deposited on the amorphous glass substrate to a cagelike pore configuration deposited on both Pt and Si(111) substrates. Such a pore configuration transition is related to the change in surface energy in association with crystal growth of the anatase phase. The mesoporous TiO_2 films deposited on a polycrystalline Pt substrate and single-crystal Si(111) wafer exhibit much higher photodegrading efficiency than that deposited on the amorphous glass substrate, as a result of the enhanced nanocrystallinity. The band-gap excitation in the former gives rise to Stokes shifted, visible broad band luminescence, which is attributed to the radiative recombination of excitons in association with the surface defects of the anatase nanocrystals. Enhancement of nanocrystallinity and preservation of the highly ordered mesostructure, which is successfully realized on polycrystalline Pt and single-crystal Si(111) substrates, prompt enhanced photocatalysis and PL behaviors.

CM060450B

(35) Li, F. B.; Li, X. Z. *Chemosphere* **2002**, *48*, 1103.